

**Figure 8.** Generator matrix  $\alpha_{si}^2$  for a polymethylene chain of 1000 bonds. Each computation uses  $b/K = 0.64$ , and the value for  $K$  is shown for each curve. The straight line segment has a slope of  $1/5$ .

is then approximated as a chain of  $n/n_c$  blobs. Changes in the environment of the chain are assumed to affect its dimensions through a change in the value for  $n_c$ . This theory predicts  $\alpha_{si}^2 = \alpha_{ri}^2 = 1$  for  $i < n_c$  and that  $d(\log \alpha_{si}^2)/d(\log i)$  and  $d(\log \alpha_{ri}^2)/d(\log i)$  are  $1/5$  for  $i > n_c$ . Modification of the simple blob theory may replace the discontinuous change from ideal to excluded volume statistics by a progressive crossover.<sup>8</sup>

Figures 7 and 8 include a line segment whose slope is  $1/5$ . Lines describing computed behavior of the subchains may have a slope of  $1/5$  at some value of  $\log i$ . However, the range of  $\log i$  over which this slope is observed is not large. Furthermore, there is no indication that the slope tends toward  $1/5$  as  $\log i$  becomes large. Indeed, the slope actually becomes negative at large  $\log i$  in Figure 7. Neither our generator matrix nor Monte Carlo calculations provide support for the blob concept. A major difficulty with simple applications of the blob concept is that they

do not properly account for the consequences of the repulsive interaction of the subchain with atoms elsewhere in the main chain. These consequences are a position dependence to the expansion of a subchain (Figures 1 and 3), a maximum for  $\alpha_{ri}^2$  at  $i < n$  (Figures 4, 6, and 7), and a pronounced sigmoid character to  $\log \alpha_{si}^2$  vs.  $\log i$  (Figures 4, 6, and 8). A maximum for  $\alpha_{ri}^2$  at  $i < n$  has also been seen with chains on a cubic lattice and recognized as being incompatible with simple applications of the blob concept.<sup>7</sup>

Subchain expansion factors could be measured by performing angle-dependent neutron scattering measurements on perturbed polymers in which the isotopic composition of the subchain was different from that of the remainder of the chain. Whether or not these subchains exhibit maximal expansion when they comprise somewhat less than the main chain will depend on the precise manner in which the isotopic labeling is accomplished. If  $\alpha_{si}^2$  is obtained from samples in which the label occurs throughout the subchain, a maximum should not be observed (Figure 8). However, if the isotopic label occurs only at the first and last atoms in the subchain, the measurement will yield  $\alpha_{ri}^2$  and a maximum is predicted (Figure 7).

**Acknowledgment.** This work was supported by National Science Foundation Research Grant PCM 78-22916.

#### References and Notes

- (1) Mattice, W. L.; Santiago, G. *Macromolecules* 1980, 13, 1560.
- (2) Mattice, W. L. *Macromolecules*, preceding paper in this issue.
- (3) Flory, P. J. *J. Chem. Phys.* 1949, 17, 303.
- (4) Farnoux, B.; Boue, F.; Cotton, J. P.; Daoud, M.; Jannink, G.; Nierlich, M.; de Gennes, P. G. *J. Phys. (Paris)* 1978, 39, 77.
- (5) Jernigan, R. L.; Flory, P. J. *J. Chem. Phys.* 1967, 47, 1999.
- (6) Flory, P. J. *Macromolecules* 1974, 7, 381.
- (7) Curro, J. G.; Schaefer, D. W. *Macromolecules* 1980, 13, 1199.
- (8) François, J.; Schwartz, T.; Weill, G. *Macromolecules* 1980, 13, 564.

## A Monte Carlo Study of the Collapse of a Polymer Chain

I. Webman and Joel L. Lebowitz\*

Departments of Mathematics and Physics, Rutgers University,  
New Brunswick, New Jersey 08903

M. H. Kalos

Courant Institute of Mathematical Sciences, New York University,  
New York, New York 10012. Received December 16, 1980

**ABSTRACT:** We study, using Monte Carlo techniques, the equilibrium configurational properties of bead-spring model polymer chains with both repulsive and attractive interactions. By varying the temperature, we represent a polymer chain in solvents with differing degrees of solubility. We find that (a) at high temperatures, corresponding to good solvents, the dependence of the chain dimension  $R$  on the number of units  $N$  follows the same power law as does a chain with purely repulsive interaction ( $R^2 \propto N^{2\nu}$ ,  $\nu \approx 0.6$ ), (b) there is a temperature  $\bar{\theta}$  in the neighborhood of Flory's  $\theta$  temperature (at which the second virial coefficient of the interaction vanishes) where there is a linear relation between  $R^2$  and  $N$  ( $\bar{\theta} - \theta$  depends on the "stiffness" of the chain), and (c) at lower temperatures the chain manifests a collapse which becomes more pronounced with increasing  $N$ . There is overall qualitative agreement between our results, experiment, and a generalized form of Flory's theory although the behavior in cases b and c appears to depend on more details of the interaction than are taken into account in the latter.

### I. Introduction

The configurations of a polymer chain in a very dilute solution are determined by the interplay between the interactions of chain segments among themselves and with the solvent. In a good solvent excluded volume effects result in a swelling of the chain relative to a random coil.

In a poor solvent, on the other hand, the polymer segments prefer self-contacts over contacts with the solvent. It is customary in polymer chain theory to represent these effects by considering an effective interaction potential  $u(r)$  between polymer segments which have a short-range repulsive part and a longer range attractive part, e.g., a

Lennard-Jones type potential. The effect of the solvent on the properties of the polymer chain can then be represented, qualitatively at least, by the temperature in the Gibbs distribution of the chain (which might not be the parameter actually varied in the experiment). In analogy to what happens in an ordinary fluid, high temperatures correspond to situations in which the effective interaction between segments is predominantly repulsive (good solvent) while low temperatures enhance the role of the attractive interactions (poor solvent).<sup>1,2</sup>

A key to understanding excluded volume effects is the observation, made by Flory,<sup>1</sup> that in a good solvent, when the chain is expanded, the polymer behaves like a low-density gas and the interaction is dominated by binary encounters between segments. It can therefore be accounted for to a great extent by the binary cluster integral

$$B(T) \equiv \int (1 - e^{-\beta u(r)}) dr \quad \beta = 1/kT \quad (1)$$

This integral is positive at high temperatures and represents then an effective excluded volume. At the  $\Theta$  temperature, defined by  $B(\Theta) = 0$  (the Boyle temperature of a fluid), there is a balance between the repulsive and attractive interactions, and the "long-range" configurational properties of the polymer chain are then similar to those of an ideal random coil. For  $T < \Theta$  the attractive interactions dominate and the chain collapses to a compact globular structure. This "coil-to-globular" transition is qualitatively analogous to the gas-liquid transition at constant chemical potential or constant pressure—in both cases the density changes sharply as the temperature is decreased.

The linear relation between the squared end-to-end distance  $R^2$  (or the squared radius of gyration  $S^2$ ) and the number of units  $N$ , characteristic of a random coil, has been experimentally verified<sup>3,4</sup> for real polymers in a  $\Theta$  solvent by neutron scattering and by viscosity data. The collapse in a poor solvent has also been observed experimentally.<sup>5-7</sup> Theoretically the collapse phenomenon was first predicted by Stockmayer<sup>8</sup> and studied both by the Flory mean field type approach<sup>9-13</sup> and by the application of renormalization group methods.<sup>2,14</sup> While there is not as yet complete agreement concerning the nature of the transition around  $T = \Theta$ , de Gennes and others have suggested that the behavior near the collapse (as the size increases) is characteristic of a tricritical point.<sup>9,11,15</sup> These studies extend Flory's original analysis for  $T \gtrsim \Theta$  by emphasizing the role of three-body interactions between chain segments at  $T \lesssim \Theta$ . This can be understood by noting that at  $T = \Theta$  the binary cluster contribution vanishes, and it is then the three-body clusters which dominate the interaction energy.<sup>16</sup> de Gennes has suggested that due to these interactions the point at which the coil is "quasi-ideal" will shift to a renormalized  $\Theta$  temperature  $\tilde{\Theta} < \Theta$  and that even at  $\tilde{\Theta}$  the internal structure of the chain will differ from that of an ideal coil.<sup>2,14</sup> At still lower temperatures in the collapsed regime, further multiple interactions become important due to the higher density of segments. The system then behaves qualitatively like a low-temperature fluid.

In the present work we study by Monte Carlo techniques the equilibrium configurational properties of bead-spring and bead-rod chains with Lennard-Jones type interactions between beads. Our results provide information about the behavior of the polymer chain in the  $\Theta$  region and on the collapse transition. Parts of this behavior have previously been studied by Monte Carlo methods on a lattice<sup>17</sup> and in continuum<sup>18</sup> and by enumeration techniques on a lattice.<sup>19</sup> Continuum models, in addition to being more re-

alistic than lattice models, also offer the possibility of varying more parameters relevant to the problem, such as the ratio between the third virial coefficient  $C(T)$  and  $B(T)$ . More generally, we feel that Monte Carlo (MC) simulations can at this stage complement both analytical theories and experimental results by offering the possibility to (a) obtain results, within known statistical errors, for a well-defined model system, (b) control the relevant parameters of the problem, and (c) probe local properties of the system that cannot be observed experimentally.

We have previously carried out Monte Carlo studies on chains with purely repulsive forces, using a Monte Carlo method with an efficient reptation dynamics to generate equilibrium configurations.<sup>20,21</sup> The same method was used in the present work for the study of chains at low temperature.

The main limitation on these simulations is imposed by the number of chain segments,  $N \lesssim 80$ , which we can do in a reasonable time. We should remember, however, that in the model there is no direct angular correlation between successive beads. Each bead can, therefore, be thought of as representing a segment of a real polymer (something de Gennes refers to as a blob). The basic assumption made here is that the large-scale physical properties of the polymer which are determined by the long-range excluded volume effects do not depend too much on the precise nature of interactions and might manifest themselves already for relatively small values of  $N$ . Indeed the power laws which characterize the  $N$  dependence of  $S^2$  and  $R^2$  at high temperature are obtained for chains as small as 5-10 beads. The limitation on the chain size, however, makes it difficult to resolve the subtle questions concerning the behavior of very long chains below the  $\Theta$  temperature, such as the order of the coil-globule transition.

This limitation, combined with the fact that the experimental information about the gross features of the system below the  $\Theta$  temperature is sparse, made it desirable to concentrate on the general behavior of the polymer chain over a wide range of temperatures around  $T = \Theta$ . We also examined the dependence of the chain properties on  $N$  and on a parameter which determines the relative contribution of larger clusters (which become important as  $T \lesssim \Theta$ ) to the free energy.

## II. Theoretical Considerations

The qualitative behavior of a polymer chain going from an expanded to a collapsed configuration as the temperature is lowered is described in a general way by an extended form of Flory's theory.<sup>9-13</sup> There is, however, no consensus at present on the quantitative aspects of these changes. We give a brief outline of some theoretical ideas before describing our numerical simulations.

**The Flory Theory.** As already noted the central idea of Flory's treatment, and of subsequent treatments, is that in a good solvent the chain is swollen so the monomer density is low and only binary interactions are important.<sup>1</sup> By combining this idea with some assumptions about the entropy of a chain, Flory<sup>1</sup> obtained his famous formula for the expansion factor  $\alpha \equiv R/N^{1/2}a$

$$\alpha^5 - \alpha^3 = p'B(T)N^{1/2}/a^3 \quad (2)$$

Here  $a$  is the distance between neighbors and  $p'$  is a numerical factor of order unity. In the mean field type theory leading to eq 2, the correlation between positions of monomers induced by the connectivity of the chain is neglected, and each monomer is assumed to see an average density  $N/R^3$  of monomers. In addition, the distribution of  $R$  is assumed to be Gaussian, as in a random chain without interactions. As the chain contracts in the

poor-solvent regime, the density of monomers increases and higher order interactions become important. Flory's approach was extended to this case by de Gennes and others<sup>9,13</sup> by incorporating the contribution of three-body clusters to the free energy. The resulting formula is

$$\alpha^5 - \alpha^3 = pB(T)N^{1/2}/a^3 + rC(T)/a^6\alpha^3 \quad (3)$$

Here  $C(T)$  is the third virial coefficient

$$C(T) \propto \int f_{12}f_{13}f_{23} d\vec{r}_1 d\vec{r}_2 d\vec{r}_3 \quad (4)$$

where

$$f_{ij} \equiv e^{-\beta u(r_{ij})} - 1$$

and  $r$  is another numerical factor of order unity.

The squared radius of gyration of the chain,  $S^2$ , is a more natural parameter than  $R^2$  below  $\Theta$ . An analogous formula to eq 3 can be defined for the ratio  $\phi \equiv S^2/(Na^2/6)$ .<sup>12</sup> We recast it here in the following form:

$$\phi^{2.5} - \phi^{1.5} - rc(T)/\phi^{1.5} = pb(T)N^{1/2} \quad (5)$$

where

$$b(T) \equiv B(T)/a^3$$

$$c(T) \equiv C(T)/a^6$$

and  $r$  and  $p$  are numerical factors which depend on the precise definition of  $B$  and  $C$ .

**Extensions of Mean Field Theory.** There have been various suggestions<sup>11,14,22</sup> for improving the approximations leading to eq 2 and 3. In particular, Kokhlov<sup>22</sup> considered corrections to the second virial coefficient due to the fact that when monomers  $i$  and  $j$  are interacting, neighboring monomers, e.g.,  $i \pm 1$  and  $j \pm 1$ , are also likely to be close enough to interact. This leads to a modified second virial coefficient  $B^*$ . Another way to improve the mean field theory in the regime  $T \leq \Theta$  was suggested by de Gennes.<sup>2,14</sup> The idea is to regard the polymer as a chain of "blobs" each made up of many monomers. The number of monomers in a blob can be chosen in such a way that the correlations between the positions of blobs are small, so that it is proper to treat the chain of blobs by a mean field approach. The parameters  $b$  and  $c$  in eq 5 now assume a different meaning, the interaction now being between blobs, but the general form of the expression will be preserved (apart from the appearance of a slowly varying logarithmic factor). This treatment is expected to be valid, however, only for very long chains. Other suggested modifications of eq 2 include replacement of the term in  $\phi^{2.5} - \phi^{1.5}$  in eq 5 by a more general function  $f(\phi)$ . The Gaussian approximation on which eq 5 is based can then be relaxed.

Several general conclusions can be drawn from these considerations concerning the behavior of polymers below the  $\Theta$  temperature:

(a) The ideal coil behavior will not occur at the temperature  $\Theta$  where the second virial coefficient of the interaction between monomers vanishes. Due to the repulsive effect of the three-body interactions, this behavior will obtain at a lower temperature, at which a "renormalized" second virial coefficient  $B^*$  vanishes.

(b) The size contraction factor  $\phi$  is a function of at least two parameters,  $\phi = \phi(bN^{1/2}, c)$ . This is in contrast with the good-solvent regime, where for very long chains  $\phi$  is a function of a single parameter,  $bN^{1/2}$ .

(c) Since for  $T \sim \Theta$ ,  $b \propto \tau = (T - \Theta)/\Theta$ , the collapse transition as a function of  $\tau$  will be more pronounced the longer the chain.

(d) For sufficiently low temperatures where  $\phi < 1$  the term  $\phi^{2.5} - \phi^{1.5}$  on the left-hand side of eq 5 might become unimportant, and a temperature regime in which the polymer is entirely collapsed with  $\phi \simeq (\tau^{2/3}N^{1/3})^{-1}$  can be expected.

In section IV we compare these conclusions with our numerical results.

### III. Description of Model and Numerical Method

Our model chain is made up of  $N$  beads located at positions  $\{r_i\} = x$  connected by springs. Any two beads along the chain interact via a Lennard-Jones potential with a cutoff, shifted to make it continuous

$$u(r_{ij}) = 4\epsilon[(\sigma/r_{ij})^{12} - (\sigma/r_{ij})^6 + (1/2^6 - 1/2^{12})] \quad (6)$$

$$r < 2\sigma$$

$$u(r_{ij}) = 0 \quad r > 2\sigma$$

The total interaction energy for a chain configuration  $x$  is then given by

$$V = \sum_{i>j} u(r_{ij}) + \frac{1}{2}A\sum(\vec{r}_{i+1} - \vec{r}_i)^2 \quad (7)$$

In our study we varied the parameters  $b$  and  $c$  defined in eq 3 by varying the parameters  $\beta = 1/kT$  and  $a^2 \equiv \langle (r_{i+1} - r_i)^2 \rangle$ , the mean-square separation between neighboring beads. The latter is achieved by varying the spring constant  $A$  in eq 7. The value of  $a^2$  is determined by the balance between the repulsive short-range interaction and the binding harmonic potential.

We have also studied chains representing a bead-rod type model. In this case, the distances  $|\vec{r}_{i+1} - \vec{r}_i|$  are kept fixed, and  $a^2 = (\vec{r}_{i+1} - \vec{r}_i)^2$ .

Near  $(\beta\epsilon)_\Theta = \Theta^{-1}$ , the root of  $B(T) = 0$ , one has  $B = v\tau$ , where  $\tau = (T - \Theta)/\Theta$  and

$$v = -\Theta \left. \frac{\partial B}{\partial T} \right|_{(\beta\epsilon)_\Theta} \quad (8)$$

For the potential given by eq 6,  $\beta\epsilon = 0.445$  and  $v = 3.75\sigma^3$  at  $T = \Theta$ . The third virial coefficient  $c$  for this potential is a relatively slowly varying function of temperature. Apart from numerical constants the normalized virial coefficients  $b$  and  $c$  of eq 5 can therefore be expressed, for  $T \simeq \Theta$ , as

$$b \sim (v/a^3)\tau \simeq \gamma\tau$$

$$c \sim (v/a^3)^2 \equiv \gamma^2 \quad (9)$$

The value of the parameter  $\gamma$  gives a measure of the strength of three-body interactions relative to that of binary interactions.<sup>10</sup> We therefore choose  $\gamma$  as the second relevant parameter in the poor-solvent regime, in addition to  $\beta\epsilon$ .

An ensemble of configurations  $x$  distributed according to the density

$$p(x) \propto \exp\{-\beta V(x)\} \quad (10)$$

was generated by a reptation Monte Carlo dynamics as follows: A configuration  $x' = \{r'_i\}$  is generated from the configuration  $x$  by the transformation

$$\vec{r}'_j = \vec{r}_{j+1} \quad j = 1, \dots, N-1$$

$$\vec{r}'_N = \vec{r}_N + \vec{s} \quad (11)$$

and the components of  $\vec{s}$ ,  $s_i$ ,  $i = 1, 2, 3$ , are determined by sampling from a Gaussian distribution

$$W_{\text{Gaussian}} \propto \exp\{-\frac{1}{2}As_i^2\} \quad (12)$$

With equal probability this transformation is carried backward; i.e.,  $\bar{r}'_1$  is obtained from  $\bar{r}$  by a similar procedure. The next configuration,  $x_{\text{new}}$ , of the Markov sequence is then taken as either  $x$  or  $x'$  according to the Metropolis criterion

$$x_{\text{new}} = x' \text{ if } \exp\{\beta[V(x) - V(x')] - (A/2)(\bar{r}_N^2 - \bar{r}'_N^2)\} > \eta$$

$$x_{\text{new}} = x \text{ otherwise} \quad (13)$$

where  $\eta$  is a random number uniform on (0,1). For the bead-rod chain a similar procedure was followed, with  $\bar{s}$  in eq 11 selected with random direction under the constraint  $|\bar{s}| = a$ . Also in this case the harmonic term does not appear in eq 12 and 7. The procedure described above obeys the detailed balance condition  $p(x') \times (\text{probability to go from } x' \text{ to } x) = p(x) \times (\text{probability to go from } x \text{ to } x')$ .

The method is an extension of the "slithering snake" idea of Mandel and Wall<sup>23</sup> for generating self-avoiding walks on lattices. It leads asymptotically to the equilibrium distribution  $p(x)$  within any region of the phase space accessible from the starting configuration. It is important to note that applying the backward transformation with probability 0.5 is essential for the validity of the detailed balance condition.

The relaxation time of the reptation dynamics described above is of the order of  $\sim N^2$  MC time steps. Equilibrium averages are obtained by dividing the total sequence of MC steps into 15–20 blocks, each block  $> N^2$ , and obtaining the final average and the standard deviation by averaging over the block averages, excluding the first couple of blocks during which the system is still in the process of equilibration. It is clear that the relaxation time is the dominant factor determining the computer running time for an experiment. Reptation MC dynamics, while not appropriate for the simulations of real dynamics, is a relatively fast procedure for the generation of equilibrium configurations of chains as compared with full molecular dynamics or even with the standard  $M(RT)^2$  method with one bead moved at random in a box. (See Ceperley et al.<sup>24</sup> for a Monte Carlo method capable of giving both equilibrium and dynamical properties of polymer chains.)

#### IV. Numerical Results and Discussion

The overall temperature and  $N$  dependence of the radius of gyration are presented in Figure 1, where  $\bar{\phi} \propto S^2/S^2(\bar{\theta})$  is plotted vs.  $\beta\epsilon$  for several values of chain lengths and for three different values of  $\gamma$ ,  $\gamma = 1.15, 0.5, 0.22$ .  $\bar{\theta} = \bar{\theta}(\gamma)$  is the temperature at which  $S^2 \propto N$  for a given  $\gamma$ . These three cases will be denoted for convenience as A, B, and C, respectively. We have employed two somewhat different models: case A corresponds to a bead-rod model (fixed distance between neighboring beads along the chain) while in cases B and C the beads are connected by springs. Analysis of the results of these two types of model for the static behavior in a good solvent indicates that the large-scale configurational properties of the chains are not affected by this difference.<sup>21</sup> Thus, only the variation of  $\gamma$  between cases A, B, and C will be considered as relevant here.

We note that in all three cases the chains contract with decreasing temperature, with the change being more abrupt for longer chains. This is consistent with the scaling properties expressed by eq 5 and suggests, by extrapolation, that for very long chains the collapse transition will occur over a very narrow temperature range (with a singular nonanalytic behavior in the limit  $N \rightarrow \infty$ ). Indeed, such behavior of a coil-to-globule transition has been recently observed experimentally by Sun et al.<sup>7</sup> for dilute

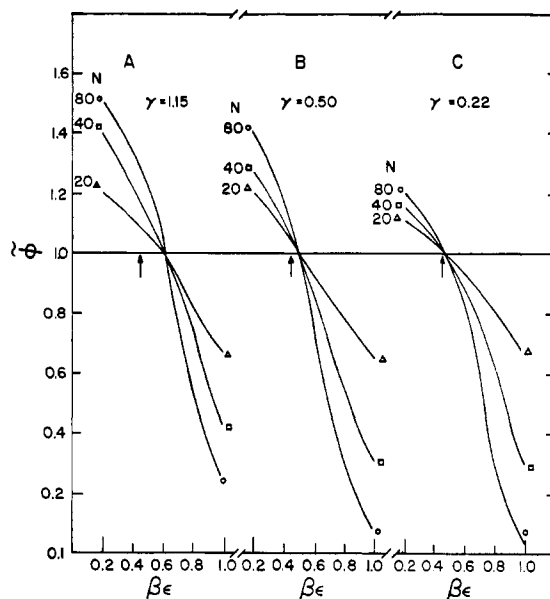


**Figure 1.** Dependence of the normalized radius of gyration  $\bar{\phi} \propto S^2/S^2(\bar{\theta})$  vs.  $\beta\epsilon$ , where  $\bar{\theta} = \bar{\theta}(\gamma)$  is the effective  $\theta$  temperature at which all the  $S^2/N$  vs.  $\beta\epsilon$  curves for a given  $\gamma$  intersect. The arrows represent the value of  $\beta\epsilon$  which corresponds to the bare  $\theta$  temperature, for which  $B(\beta\epsilon) = 0$ .

polystyrene solution in cyclohexane. The value of  $S^2$  for a chain of molecular weight  $M_w = 2.6 \times 10^7$  varied by an order of magnitude over a temperature range of about 1 K while smaller chains,  $M_w = 2.9 \times 10^3$ , showed a relatively slow variation of  $S^2$  with temperature.<sup>6</sup>

While the qualitative behavior of  $\bar{\phi}(\beta\epsilon, N, \gamma)$  presented in Figure 1 is similar for all values of  $\gamma$ , the value of  $\beta\epsilon$  at which the curves for different  $N$  intersect, i.e., at which  $S^2 \propto N$ , depends on  $\gamma$ , the effective  $\theta$  temperature,  $\bar{\theta}$ , being lowered relative to the zero-order or "bare"  $\theta$  temperature, defined by  $B(\theta) = 0$ , for higher values of  $\gamma$ . The numerical results are roughly consistent with the linear  $\gamma$  dependence of  $\bar{\theta} - \theta$ , given by eq 5,  $\bar{\theta} - \theta \propto \gamma/N^{1/2}$ , but  $\bar{\theta} - \theta$  does not seem to depend on  $N$ . This may be interpreted as follows: Near  $\bar{\theta}$ , the most important nonbinary cluster terms in the free energy are those for which nearest-neighbor monomers along the chain interact with a third monomer. Such connected many-body terms do not appear at low density for an ordinary gas of atoms. They should be proportional to  $N\rho((v/a^3)^2)$  so that  $B(T)$  in eq 3 should be replaced to first order in  $\gamma$  by

$$B^*(T) \simeq B(T) + \eta\gamma$$

where  $\eta$  is a numerical factor. This leads to an  $N$ -independent correction to  $\bar{\theta}$ .

In Figure 2 we plot the  $N$  dependence of  $S^2$  for case A at three temperatures. The lines on the log-log plots have slopes of 1.2, 1.0, and 0.66 for  $\beta\epsilon = 0.2, 0.6$ , and  $0.8$ , respectively. We discuss these separately.

(i) The excluded volume behavior at the highest temperature,  $\beta\epsilon = 0.2$ , is characterized by  $S^2 \propto N^{2\nu}$ , with  $\nu \simeq 0.6$ , in agreement with results for bead-rod chains with purely repulsive interactions. The amplitude of the  $S^2$  vs.  $N^{2\nu}$  power law is, however, different. For purely repulsive potentials, similar to eq 6 but without the attractive well,  $S^2 \simeq 0.15a^2N^{2\nu}$ ,<sup>17</sup> while in the present case  $S^2 \simeq 0.09a^2N^{2\nu}$ . This indicates that the value of the excluded volume exponent is insensitive to the specific shape of the interaction potential and thus adds support to the idea of the universality of this exponent. The amplitude, on the other hand, depends, as it should, on the details of the potential.

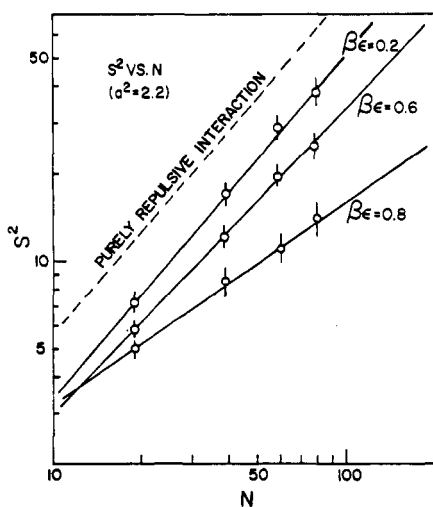


**Figure 2.** log-log plot of  $S^2$  vs.  $N$  for temperatures above and below  $\bar{\theta}$  and at  $T = \bar{\theta}$  ( $\beta\epsilon = 0.2, 0.8,$  and  $0.6,$  respectively). The slopes of the straight lines are 1.2, 1.0, and 0.66.

(ii)  $\beta\epsilon \cong 0.6$  corresponds to the effective  $\bar{\theta}$  temperature,  $\bar{\theta}$ , where the cancellation between the repulsive and attractive effects leads to a linear  $S^2$  vs.  $N$  behavior.

(iii) The approximate relationship  $S^2 \sim N^{0.66}$  at  $\beta\epsilon = 0.8$  suggests an  $N$ -independent average density of beads,  $\rho \sim N/S^3$ . In terms of the blob picture of de Gennes,<sup>14</sup> the partially collapsed chain is viewed as made up of relatively close packed noninterpenetrating blobs whose size does not depend on  $N$ ; their number is therefore proportional to  $N$ . (These blobs cannot be identified with individual beads since at  $\beta\epsilon = 0.8$  the average density of the chain is much lower than that of a fully collapsed chain.) However, the fact that the  $S^2 \cong N^{0.66}$  law is only seen in a narrow temperature range calls for some caution in the interpretation and indicates that further studies are needed.

In Figure 3 we present in more detail the behavior in the collapse transition region;  $\log \bar{\phi}$  is plotted vs.  $\log |\bar{B}|$ ,  $\bar{B} \equiv B(T) - B(\bar{\theta})$ , for different values of  $N$  and  $\gamma$ . ( $\bar{B} \propto (T - \bar{\theta})/\bar{\theta}$  for  $(T - \bar{\theta})/\bar{\theta} \ll 1$ . In our case  $\bar{B}$  is in the range  $1 < |\bar{B}| < 5$  and there are some deviations from this linear relation.) Note that the dependence of  $\bar{\theta}$  on  $\gamma$  apparent in Figure 1 is "transformed out" in this representation. Also, if  $\bar{\phi}$  depended on  $N$  and  $\bar{B}$  through a relationship of the type  $\bar{\phi} \sim \bar{\phi}[(\bar{B}/a^3)f(N), \dots]$  as predicted by mean field theory, then plots of  $\log \bar{\phi}$  vs.  $\log |\bar{B}|$  for different  $N$  would have the same shape and just be displaced along the  $x$  axis. This representation thus highlights the detailed shape of  $S^2$  vs.  $\bar{B}$  curves in the transition region. The following qualitative features are noticeable:

(a) For a fixed value of  $N$  the average slope in the transition region is larger for smaller values of  $\gamma$ .

(b) For a fixed value of  $\gamma$  the transition is somewhat more pronounced with increasing  $N$ . As already mentioned, this implied some deviation from a scaling relation of the type

$$\bar{\phi} \sim \bar{\phi}[(\bar{B}/a^3)f(N), \dots] \quad (14)$$

(c) The mean field result,  $\bar{\phi} \sim |\bar{B}|^{-2/3}$ , does not appear in the range of  $\bar{B}$  studied here for most values of  $N$  and  $\gamma$ . For the case of  $N = 40$  and  $\gamma = 1.15$  the slope of  $\log \bar{\phi}$  vs.  $\log \bar{B}$  is close to  $-0.66$  but that might be fortuitous.

We also plot in Figure 3 the results obtained by solving mean field eq 5. The parameter  $b(T)$  in eq 5 was identified with  $\bar{B}(T)/a^3$  since in eq 5 at  $b = 0$ ,  $\bar{\phi} = \text{const}$ , or  $S^2 \propto N$ . The form of eq 5 used was

$$\bar{\phi}^{2.5} - \bar{\phi}^{1.5} - r'\gamma^2/\bar{\phi}^{1.5} = p'[\bar{B}(T)/a^3]N^{1/2} \quad (15)$$

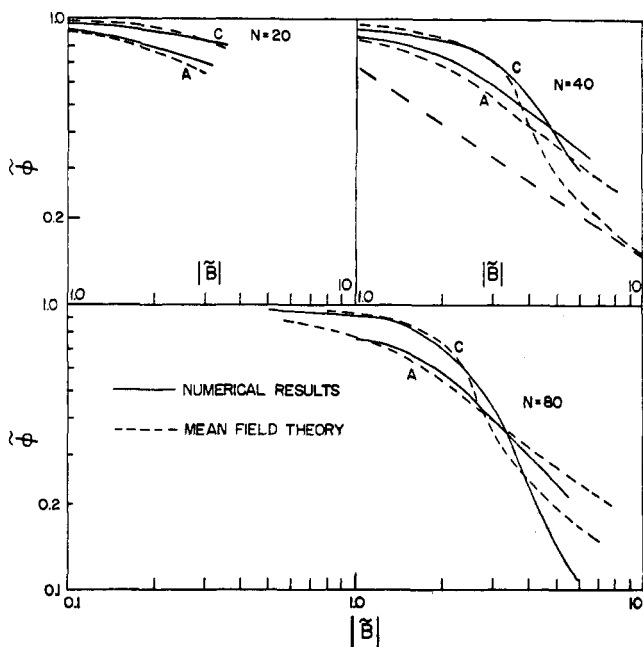


**Figure 3.** log-log plots of  $\bar{\phi}$  vs.  $|\bar{B}| \propto |B - B(\bar{\theta})|$ . The numerical results (solid lines) are compared with the solution of eq 15 (dashed lines). The dashed lines correspond to a  $\bar{\phi} \propto |\bar{B}|^{-2/3}$  dependence.

with  $p' = 0.23$  and  $r' = 0.44$  for case A ( $\gamma = 1.15$ ) and  $p' = 0.23$  and  $r' = 0.93$  for case C ( $\gamma = 0.22$ ) chosen for optimal fit to our MC results.

Note that the shape of the  $\log \bar{\phi}$  vs.  $\log |\bar{B}|$  curves obtained from eq 15 depends only on the parameter  $r'\gamma^2$ . Varying  $p'$  or  $N$  just shifts this curve along the  $\log |\bar{B}|$  axis. The degree of fit does not seem to be very sensitive to the values of  $r'$  and  $p'$ .

The general form of the curves  $\log \bar{\phi}$  vs.  $\log |\bar{B}|$  obtained from eq 15 agrees qualitatively with the numerical results but not in some of the details of the transition. Both the theory and our results show a more pronounced transition for smaller values of  $\gamma$ , where the role of three-body clusters is least significant. Also, both mean field and numerical results show a displacement of the onset of the sharp transition region to higher values of  $\log |\bar{B}|$  for smaller  $N$  values. However, while eq 15 predicts the scaling property  $\bar{\phi} = \bar{\phi}(|\bar{B}(T)|N^{1/2}, \dots)$ , our results deviate from it somewhat. This deviation is expressed in a somewhat more abrupt transition on the log-log scale for larger values of  $N$ . Also, the mean field results for case C show a region of rather pronounced collapse transition followed by a  $|\bar{B}(T)|^{-0.66}$  type behavior at lower temperatures, which is not generally found in our result.

**Comparison with Experiment.** As mentioned above, Sun et al.<sup>7</sup> have studied the collapse transition for polystyrene molecules of high molecular weight,  $M_w = 2.6 \times 10^7$ , in cyclohexane. Their log-log plot of  $S^2$  vs.  $T - \bar{\theta}$  is generally similar to our results plotted in Figure 3, where the best agreement is with the chain of  $N = 80$  for case C. A more detailed comparison of the two curves reveals that the experimental results are characterized by a rather abrupt transition followed by a  $\sim |T - \bar{\theta}|^{-0.66}$  behavior at lower temperatures. Our results show a somewhat more gradual collapse and the  $(T - \bar{\theta})^{-0.66}$  dependence is not clearly manifest. Sun et al. fit their result to a solution of an equation analogous to eq 15, with  $(r'\gamma^2) = 0.027$  (vs.  $(r'\gamma^2) \sim 0.04$  for our results), i.e., with a still lower value of  $\gamma$  than ours. The number of statistical units, analogous to the beads in our chain, in a polystyrene molecule of  $M_w \sim 2.6 \times 10^7$  is of the order of  $10^4$ , i.e., much higher than

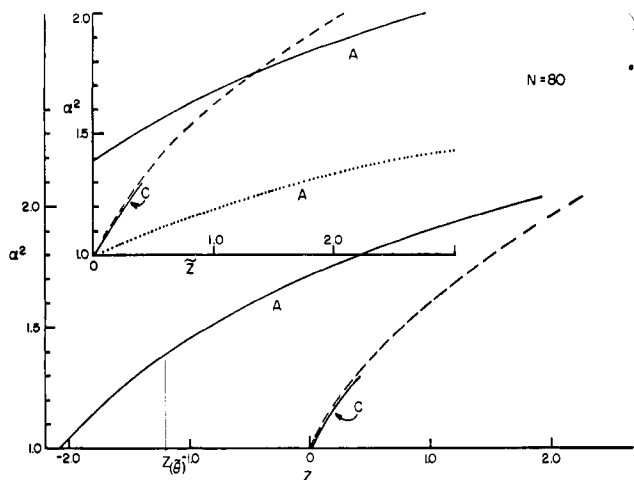


**Figure 4.** Expansion factor of the squared end-to-end distance,  $\alpha^2 \propto R^2/Na^2$ , plotted vs.  $Z \propto (3/2\pi)^{3/2}B(\beta\epsilon)N^{1/2}a^3$  for cases A and C for  $N = 80$ . The dashed line represents numerical results for purely repulsive interactions. Inset:  $\alpha^2$  plotted vs.  $\tilde{Z} \propto (3/2\pi)^{3/2}|\tilde{B}(T)|N^{1/2}/a^3$  (solid line) and  $R^2/R^2(\tilde{\theta})$  plotted vs.  $\tilde{Z}$  (dotted line) for cases A and C. The dashed line represents the results for purely repulsive interactions.

our  $N = 80$ . It thus appears from this comparison and from our data for different values of  $N$  that longer chains correspond in some way to smaller values of  $\gamma$ .

A possible argument for this behavior, using de Gennes' procedure of renormalization along the chain may be made as follows: If the chain is viewed as made up of subchains or blobs of  $n$  units each, one can define  $\tilde{b}_n$  and  $\tilde{c}_n$  as the second and third virial coefficients for the interactions between blobs. de Gennes argues that  $\tilde{c}_n$  is a decreasing function of  $n$  at  $T \lesssim \tilde{\theta}$ .<sup>14</sup> As shown in ref 3, the mean field formula, eq 5, should be applied to the sequence of blobs rather than to the sequence of monomers. When a macromolecule of size  $N_m$  is compared with a model chain of  $N$  beads, each bead represents a blob of  $n = N_m/N$  units. If in the limit  $n \rightarrow \infty$ ,  $\tilde{c}_n \rightarrow c^*$ , then for molecules that are not very long a higher value of  $N_m$  might indicate a lower value of  $\tilde{c}$  (or lower value of  $\gamma$ ). Further numerical studies would be required to study this effect. The experimental results of Nierlich et al.<sup>6</sup> for short macromolecules ( $M_w = 2.9 \times 10^4$ ,  $N_m \sim 20$ ) show a gradual contraction instead of a sharp collapse. It would be worthwhile to study this transition experimentally over a wide range of  $M_w$  and  $N_m$  in order to clarify this important point.

**The Crossover Regime:**  $T \gtrsim \tilde{\theta}$ . Recently we discussed the dependence of the size,  $R^2$  or  $S^2$ , of a chain with purely repulsive interactions on the strength of the excluded volume interaction (as expressed by the binary cluster integral  $B$  defined by eq 1).<sup>21</sup> Here we examine the crossover from quasi-ideal coil behavior in the  $\theta$  region to excluded volume behavior at higher temperatures for the more general interactions studied in the present work.

The dependence of the expansion factor of the squared end-to-end distance  $\alpha^2 \propto R^2/Na^2$  on  $Z \propto (3/2\pi)^{3/2}B(\beta\epsilon, \sigma)N^{1/2}/a^3$  for fixed  $N$ ,  $N = 80$ , for case A and case C at temperatures  $T > \tilde{\theta}$  and for purely repulsive interactions is shown in Figure 4. In the case of the purely repulsive interaction, the value of  $B$  was varied by varying  $\sigma/a$  while  $\beta\epsilon$  was kept fixed, whereas in the present case  $B$  is varied by varying  $\beta\epsilon$  while  $\sigma/a$  is fixed. It is interesting to note that  $\alpha^2(Z, N = 80)$  for case C agrees closely with  $\alpha^2(Z, N = 80)$  for the repulsive interaction in the region  $0 < Z \leq 0.5$ . For case A, however,  $\alpha^2(Z, N = 80)$  vs.  $Z$  is markedly different. It might be more appropriate to compare these two cases when  $\alpha^2$  is plotted vs.  $\tilde{Z} \propto [(3/2\pi)^{3/2}|\tilde{B}(T)|]N^{1/2}/a^3$ .

This plot is shown in the inset. An even more general comparison between these cases, plots of  $R^2/R^2(\tilde{\theta})$  vs.  $\tilde{Z}$  is also presented. In all these representations there is a significant difference between the crossover from  $\theta$  behavior to excluded volume behavior in the case of repulsive interactions and in case A. This difference might be due to several factors, which are probably related to each other:

(a) Interactions between beads that are next nearest neighbors along the chain. This leads to correlations between the directions of subsequent links of the chain such that  $\langle \cos \delta \rangle \propto (\sigma/a)^2 \sim \gamma^{2/3}$  (where  $\delta$  is the angle between subsequent links). This effect would be more pronounced in case A than in case C, would result in an expansion of the chain near  $T \sim \tilde{\theta}$ , but would not affect the linear  $N$  dependence of  $R^2$  in this region. It is interesting in this context to compare our case A (with  $(\sigma/a)^2 = 0.45$  and  $(R^2/Na^2)|_{T=\tilde{\theta}} = 1.4$ ) with the results of ref 15 (where  $(\sigma/a)^2 = 1$  and  $(R^2/Na^2)|_{T=\tilde{\theta}} = 1.7$ ).

(b) Three-body clusters of beads  $i, j, k$  such that, for example,  $|i - j| = 1$  and  $|i - k|, |j - k| \gg 1$  (or higher order terms of a similar nature). The contribution of such terms to the free energy is of the order of  $\gamma^2 \sim (\sigma/a)^6$ . As discussed above these effects could, in principle, be accounted for by a definition of a renormalized cluster integral  $B^* = B^*(B, \gamma, \beta\epsilon, \dots)$ . The dependence of  $\alpha^2$  on  $B^*$  would be different from the dependence on  $B$ , and  $\alpha^2(B^*N^{1/2}/a^3, \dots)$  might then be similar for the three cases compared.

(c) "Long-range" three-body clusters of beads  $i, j, k$  such that  $|i - j|, |i - k|, |j - k| \gg 1$ . These terms are also of order  $\gamma^2 \sim (\sigma/a)^6$ .

All three of these contributions vanish in the limit  $\sigma/a \rightarrow 0$ , which could explain why case C agrees quite well with the repulsive case for  $Z \leq 0.4$ . In this  $Z$  region,  $(\sigma/a)^3 \ll 1$  in both cases. For case A, on the other hand,  $(\sigma/a)^3 \sim 1$  for all  $Z$  values.

In ref 21 we compared the crossover function  $\psi(z)$ , which is the limit of  $\alpha^2(Z, N)$  as  $(\sigma/a)^3 \rightarrow 0$ ,  $N \rightarrow \infty$  such that  $Z \propto (\sigma/a)^3 N^{1/2}$  remains finite, deduced from our simulations with experimental data for polystyrene molecules in cyclohexane. We found good agreement between our results and the experimental data. This suggests that three-body interactions, short-range correlations, etc. do not affect significantly the asymptotic behavior of very long flexible chains. It seems possible that even for bead chains with  $\sigma/a \sim 1$  the universal crossover behavior will be recovered in the limit of very large  $N$ .

**Acknowledgment.** This work was supported in part by AFOSR Grant No. 78-3522 and by U.S. DOE Contract DE-AC02-76ER03077. Acknowledgment is also made to the donors of the Petroleum Research Fund, administered by the American Chemical Society, for partial support of this research.

## References and Notes

- Flory, P. J. "Principles of Polymer Chemistry"; Cornell University Press: Ithaca, N.Y., 1971. *Science* 1977, 188, 1268.
- de Gennes, P. G. "Scaling Concepts in Polymer Physics"; Cornell University Press: Ithaca, N.Y., 1979.
- Chinai, S. N.; Samuels, R. J. *J. Polym. Sci.* 1956, 19, 463.
- Farnoux, B. *J. Phys. (Orsay, Fr.)* 1978, 39, 77.
- Slagowski, E. L.; Tsai, B.; McIntyre, D. *Macromolecules* 1976, 9, 687.
- Nierlich, M.; Cotton, J. P.; Farnoux, B. *J. Chem. Phys.* 1978, 69, 1379.
- Swislow, G.; Sun, S. T.; Nishio, I.; Tanaka, T. *Phys. Rev. Lett.* 1980, 44, 796. Sun, S. T.; Nishio, I.; Swislow, G.; Tanaka, T., preprint.
- Stockmayer, W. H. *Makromol. Chem.* 1960, 35, 54.
- de Gennes, P. G. *J. Phys., Lett. (Orsay, Fr.)* 1975, 36, L-55.
- Moore, M. *J. Phys. A* 1977, 10, 305.
- Lifshitz, I. N.; Grosberg, A. Y.; Khokhlov, A. R. *Rev. Mod. Phys.* 1978, 50, 683.

- (12) Oono, Y.; Oyama, T. *J. Phys. Soc. Jpn.* 1978, 44, 301.  
 (13) Sanchez, I. C. *Macromolecules* 1979, 12, 980 and additional references therein.  
 (14) de Gennes, P. G. *J. Phys. B* 1978, 9, L-299.  
 (15) Stephen, M. J. *Phys. Lett. A* 1975, 53, 363.  
 (16) Orofino, T. A.; Flory, P. J. *J. Chem. Phys.* 1957, 26, 1067.  
 (17) Mazur, J.; McCrackin, F. L. *J. Chem. Phys.* 1968, 49, 648. McCrackin, F. L.; Mazur, J.; Guttman, C. L. *Macromolecules* 1973, 6, 859.  
 (18) Baumgartner, A. *J. Chem. Phys.* 1980, 72, 871.  
 (19) Rapaport, D. C. *Macromolecules* 1974, 7, 64. *Phys. Lett. A* 1974, 48, 339. *J. Phys. A* 1977, 10, 637.  
 (20) Webman, I.; Lebowitz, J. L.; Kalos, M. H. *J. Phys. (Orsay, Fr.)* 1980, 41, 579.  
 (21) Webman, I.; Lebowitz, J. L.; Kalos, M. H. *Phys. Rev. B* 1981, 23, 316.  
 (22) Khokhlov, A. R. *J. Phys. (Orsay, Fr.)* 1977, 38, 845.  
 (23) Wall, F. T.; Mandel, F. *J. Chem. Phys.* 1971, 63, 4592.  
 (24) Ceperley, D.; Kalos, M. H.; Lebowitz, J. L. *Phys. Rev. Lett.* 1978, 41, 313. *Macromolecules*, this issue.

## Toward a Molecular Theory of the Trommsdorff Effect

Thomas J. Tulig and Matthew Tirrell\*

Department of Chemical Engineering and Materials Science, University of Minnesota, Minneapolis, Minnesota 55455. Received March 31, 1981

**ABSTRACT:** A theory for the kinetics of high-conversion autoaccelerating free radical polymerization, incorporating the reptation model of de Gennes for polymer diffusion, is presented. Earlier models of various aspects of the Trommsdorff effect are reviewed and several weaknesses pointed out. These approaches have been empirical in the sense that diffusion behavior has usually been put in an ad hoc manner flexible enough so that it could be adjusted to fit experimental data. The present model uses classical diffusion-controlled reaction kinetics (the Smoluchowski equation) to relate the termination rate constant to the diffusion constant of the growing radical. The best current theory for polymer diffusion is then included in the kinetic model. The model is shown to fit data on conversion vs. time and molecular weight vs. conversion up to 70 or 75% conversion. Examination of some data due to Brooks shows that the dependence of the termination rate constant on molecular weight is consistent, at high molecular weight, with the inverse square chain length dependence expected from this reptation-based kinetic model. The model suggests several new experimental approaches to a better understanding of the molecular dynamics of polymerizing media.

### Introduction

The course of free radical polymerization carried out in both concentrated solution and bulk monomer has been a matter of study for over 3 decades. From the vast array of published experimental data<sup>1-17</sup> it is well-known that classical low-conversion free radical kinetics<sup>18,19</sup> do not apply over the entire conversion range in concentrated polymerizing systems. In particular, many such polymerizations exhibit a large autoacceleration of the rate of polymerization with an associated increase in the molecular weight of the polymer produced in media on the order of 20-30% in polymer content, even under isothermal conditions. This autoacceleration, known as the Trommsdorff<sup>1</sup> or "gel" effect, is the result of a drastic decrease in the rate of chain termination steps due to severe diffusional limitations.

Diffusion theory of polymers has advanced considerably in the past 10 years. The purpose of the present work is to use some of these advances to put the molecular understanding of the Trommsdorff effect on a more solid footing. Simple empirical methods have been used to describe such polymerization kinetics by correlating an "apparent" termination constant with various system parameters, such as conversion, temperature, and free volume.<sup>20-22</sup> More recently, two approaches have evolved which attempt to relate high-conversion polymerization and the "gel" effect to some feature of the underlying physics of the problem. One approach, used by Turner and co-workers,<sup>23-28</sup> deals only with the onset of the autoacceleration. A point of departure of experimental data from classical dilute-solution kinetics (there is a certain arbitrariness here) is identified with a "critical" polymer concentration,  $C_{crit}$ , at which the onset of the gel effect is defined to occur. Theories of polymer dynamics and extensive rheological data due to Graessley, Bueche, Onogi, and others<sup>29-32</sup> have attributed observed changes in the concentration and molecular weight dependence of poly-

mer dynamic properties such as viscosity, modulus, and compliance when crossing from dilute to more concentrated solution to the onset of "entanglements"; moreover, they have established that the onset of such "entangled" behavior obeys an equation of the form

$$K = C_{crit} \bar{M}_{crit}^a \quad (1)$$

where  $C_{crit}$  is the polymer concentration,  $\bar{M}_{crit}$  is some average molecular weight, and  $a$  and  $K$  are constants, with  $0.5 \leq a \leq 1$ . Turner et al.<sup>23-28</sup> suggest that the onset of the gel effect be identified with either the onset of molecular overlap ( $a = 0.5$ ) or the onset of "entanglement" ( $a = 1$ ) in the polymerizing mixture, and the dependence of  $C_{crit}$  on the molecular weight of the polymer produced is fit to the form of eq 1.

The most systematic experimental studies of this dependence are those of O'Driscoll, Wertz, and Husar,<sup>33</sup> Abuin and Lissi,<sup>34</sup> Lachinov et al.,<sup>35</sup> and Lee and Turner.<sup>24-28</sup> O'Driscoll et al.<sup>33</sup> studied the polymerization of styrene and found that their data fit eq 1 with  $a = 1$ , using the number-average molecular weight of the polymer produced for  $\bar{M}$  ( $\bar{M} = \bar{M}_n$ ). They also observed that the value of  $K$  obtained was lower than that observed in rheological measurements on the same system. Abuin and Lissi<sup>34</sup> used their own data as well as data due to Naylor and Billmeyer,<sup>14</sup> Schulz,<sup>9</sup> and Balke and Hamielec<sup>2</sup> on MMA polymerization and found that  $a \approx 0.5$  for high number-average degrees of polymerization, while for low degrees of polymerization the data did not fit eq 1. Lachinov et al.<sup>35</sup> studied methyl methacrylate (MMA) and butyl methacrylate (BMA) and found  $a = 0.53$  for MMA and  $a = 0.25$  for BMA. Lee and Turner<sup>24-28</sup> studied MMA, styrene, and vinyl acetate and found  $a = 0.4, 0.35,$  and  $0.34$ , respectively.

The major conclusion which can be drawn from this work is that the onset of the gel effect does correlate with some change in the character of polymer solution prop-